

The Effects of Antimony Addition on the Microstructural, Mechanical, and Thermal Properties of Sn-3.0Ag-0.5Cu Solder Alloy



PHAIROTE SUNGKHAPHAITON and THAWATCHAI PLOOKPHOL

In this study, we investigated the effects produced by the addition of antimony (Sb) to Sn-3.0Ag-0.5Cu-based solder alloys. Our focus was the alloys' microstructural, mechanical, and thermal properties. We evaluated the effects by means of scanning electron microscopy (SEM), energy dispersive X-ray spectroscopy (EDX), differential scanning calorimetry (DSC), and a universal testing machine (UTM). The results showed that a part of the Sb was dissolved in the Sn matrix phase, and the remaining one participated in the formation of intermetallic compounds (IMCs) of $\text{Ag}_3(\text{Sn,Sb})$ and $\text{Cu}_6(\text{Sn,Sb})_5$. In the alloy containing the highest wt pct Sb, the added component resulted in the formation of SnSb compound and small particle pinning of $\text{Ag}_3(\text{Sn,Sb})$ along the grain boundary of the IMCs. Our tests of the Sn-3.0Ag-0.5Cu solder alloys' mechanical properties showed that the effects produced by the addition of Sb varied as a function of the wt pct Sb content. The ultimate tensile strength (UTS) increased from 29.21 to a maximum value of 40.44 MPa, but the pct elongation (pct EL) decreased from 48.0 to a minimum 25.43 pct. Principally, the alloys containing Sb had higher UTS and lower pct EL than Sb-free solder alloys due to the strengthening effects of solid solution and second-phase dispersion. Thermal analysis showed that the alloys containing Sb had a slightly higher melting point and that the addition amount ranging from 0.5 to 3.0 wt pct Sb did not significantly change the solidus and liquidus temperatures compared with the Sb-free solder alloys. Thus, the optimal concentration of Sb in the alloys was 3.0 wt pct because the microstructure and the ultimate tensile strength of the SAC305 solder alloys were improved.

<https://doi.org/10.1007/s11661-017-4439-5>

© The Minerals, Metals & Materials Society and ASM International 2017

I. INTRODUCTION

OVER the past several years, Sn-Pb alloys have been typically used in conventional soldering processes owing to the unique properties and low cost of the materials.^[1] However, medical studies have shown that Pb is a heavy metal toxin that can damage the kidneys, liver, blood, and central nervous system.^[2,3] Therefore, alternative Pb-free solder alloys with the right balance of thermal, mechanical, and soldering properties have attracted the interest of several research groups.^[4] Recently, studies of high Ag-content Sn-Ag-Cu (SAC) solder alloys have increased exponentially since their generally superior mechanical properties and relatively good solderability

make these alloys the most promising candidates in microelectronics applications.^[5] However, these alloys have some drawbacks, including short creep rupture lifetimes. In addition, the formation of Ag_3Sn and Cu_6Sn_5 intermetallic compounds (IMCs) in the solder matrix impairs the mechanical performance of the solder joints leading to failure under stressed conditions in actual service.^[6]

For this reason, some metal additives, such as Bi, Sb, In, Co, Ge, Ni, Ga, and nanoparticles, have been introduced into SAC solder alloys in order to refine the microstructures and to inhibit the formation of IMCs.^[7–10] Interestingly, it has also been reported that the addition of Sb improved mechanical properties of the alloys, mainly due to the solid-solution hardening and particle hardening effects of Sb. The formation of SnSb in the β -Sn matrix phase, and the presence of Sb could suppress the coarsening of the β -Sn and refine the IMCs, thus improving the mechanical and thermal properties of the Sn-based solder alloys.^[11–15] Chen and Li reported that the addition of 1.0 wt pct Sb into Sn-3.5Ag-0.7Cu solders led to the formation of $\text{Ag}_3(\text{Sn,Sb})$ IMC layers and decreases in the thickness and grain size of the IMCs. Greater than this amount,

PHAIROTE SUNGKHAPHAITON is with the Department of Materials Science and Technology, Faculty of Science, Prince of Songkla University, 90112 Hat Yai, Thailand. Contact e-mail: phairote.s@psu.ac.th THAWATCHAI PLOOKPHOL is with the Department of Mining and Materials Engineering, Faculty of Engineering, Prince of Songkla University, 90112 Hat Yai, Thailand. Manuscript submitted March 27, 2017.

Article published online December 20, 2017

the thickness of the IMCs increased slightly. Adding Sb into Sn-3.5Ag-0.7Cu solders increased the activation energy, reduced the atomic diffusion rate, and inhibited the excessive growth of the IMCs.^[12,15] Mahmudi and Mahin-Shirazi reported that the addition of 1.5 wt pct Sb into Sn-3.5Ag binary solder alloys resulted in increases in both the ultimate tensile strength (UTS) and ductility of solder alloys. The increased strength of the alloy was attributed to the solid-solution hardening effects of Sb in the β -Sn matrix phase.^[11] The thermal properties of solder alloys are also important in the soldering process, and binary phase diagrams were constructed to understand the melting behavior of solder alloys by including the following design criteria: (1) the liquidus temperature should be as close as possible to 183 °C (Sn-37Pb), in order to avoid changes to the manufacturing processes; (2) the solidus temperature should be as close as possible to the liquidus temperature; and (3) the solidus temperature should be significantly higher than the maximum operating temperature during soldering.^[16] Lee et al. reported that the additions of 1.0, 1.5, and 2.0 wt pct Sb into binary Sn-3.5Ag solders increased the solidus and liquidus temperatures of the solders. The addition of 1.5 wt pct Sb produced the narrowest range between the solidus and liquidus temperatures, which is a desirable result for the real-world soldering processes.^[17] For ternary solder alloys, the melting behavior of Sn-Ag-Cu solder was determined to be closely related with a clear eutectic melting onset at 217 °C. The melting range had a very small liquid/solid or pasty range (less than about 3 °C) for a wide range of solder compositions.^[18] The experimental report of Moon et al. confirmed that the liquid phase of ternary alloys (Sn-3.5Ag-0.9Cu) occurs at about 217.2 °C.^[19] Therefore, in this research, we investigated the influences of the addition of Sb on the microstructural, mechanical, and thermal properties of Sn-3.0Ag-0.5Cu solder alloy for use in the electronics industry.

II. EXPERIMENTAL PROCEDURES

A. Preparation of Samples

Five different solder alloys were prepared with the following nominal compositions (wt pct): Sn-3.0Ag-0.5Cu, Sn-3.0Ag-0.5Cu-0.5Sb, Sn-3.0Ag-0.5Cu-1.0Sb, Sn-3.0Ag-0.5Cu-2.0Sb, and Sn-3.0Ag-0.5Cu-3.0Sb. The solder alloys were produced using Sn, Ag, Cu, and Sb of a purity ≥ 99.95 pct. The component metals were melted in an electric furnace at 673 K (400 °C) and held at that temperature for 24 hours to complete their dissolution. Then the temperature was lowered to 543 K (270 °C). The melt was poured into a steel mold preheated to 493 K (220 °C). The specimens were solidified in a mold-cooled system, while their temperature was monitored *via* type K thermocouples and recorded by data acquisition (DAQ). Before examining the alloys in order to characterize their microstructures, the specimens were cut into small pieces, molded,

polished, and etched for 5 seconds using a solution mixture of 5 pct HNO₃, 92 pct CH₃OH, and 3 pct HCl.

B. Metallographic Observation

The microstructure of the specimens was characterized by scanning electron microscopy (SEM, Quanta 400, FEI). Phase identification was based on energy dispersive X-ray spectroscopy (EDX). Differential scanning calorimetry (DSC, NETZSCH, DSC 200 F3 Maia) was employed to analyze the melting and freezing processes of the solder alloys, and the chemical compositions of the solder alloys were characterized by X-ray fluorescence spectroscopy (XRF, PW2400, PHILIPS, see Table I).

C. Mechanical Testing

The tensile specimens were cast into dumbbell-shaped test specimens with a gage length of 25 mm and a gage section diameter of 5 mm (Figure 1). The tensile tests were carried out using a universal testing machine (UTM) at a constant rate of speed of 1.5 mm/min at ambient temperature. Three specimens were tested for each condition of the mechanical properties. In this way, we obtained average testing data.

III. RESULTS AND DISCUSSION

A. Mechanical Properties of Solder Alloys

1. Tensile properties

The stress-strain curves of SAC305, SAC305 + 0.5 Sb, SAC305 + 1.0Sb, SAC305 + 2.0Sb, and SAC305 + 3.0Sb solder alloys in Figure 2 show that, as the Sb content increased from 0.5 to 3.0 pct, the strength of the alloy increased, and its ductility decreased. Figures 3 and 4 show test results for the ultimate tensile strength

Table I. Chemical Composition of Solder Alloys

| Solder Alloys | Composition (At. Pct) | | | |
|----------------|-----------------------|------|------|---------|
| | Ag | Cu | Sb | Sn |
| SAC305 | 3.68 | 0.41 | — | balance |
| SAC305 + 0.5Sb | 3.67 | 0.48 | 0.70 | balance |
| SAC305 + 1.0Sb | 3.29 | 0.53 | 1.01 | balance |
| SAC305 + 2.0Sb | 3.46 | 0.44 | 2.17 | balance |
| SAC305 + 3.0Sb | 3.44 | 0.48 | 3.20 | balance |

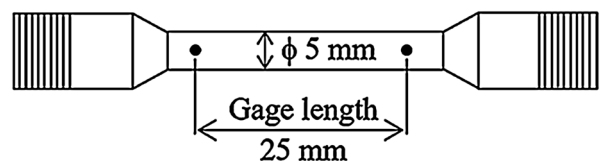


Fig. 1—Schematic of a tensile specimen.

(UTS) and elongation (pct EL) of the solder alloys. SAC305 achieved 29.21 MPa UTS and 48 pct EL, but upon adding 0.5 to 3.0 wt pct Sb to SAC305 solder alloys, the UTS increased up to a maximum value of 40.44 MPa, while the pct EL decreased to a minimum of 25.43 pct. According to previous reports, increasing the tensile strength improved the shear and creep properties of solder alloys.^[20,21] In contrast, the subsequent reduced ductility negatively influenced the strength and failure mode of the solder joint. Poor ductility reduced performance and induced a brittle solder interface.^[22,23] The gain in ultimate tensile strength and loss of ductility were attributed to the solid-solution-strengthening and the second-phase dispersion-strengthening effects of Sb in the β -Sn matrix phase^[11,15,24] and the formations of $\text{Ag}_3(\text{Sn,Sb})$ and $\text{Cu}_6(\text{Sn,Sb})_5$ IMCs on the grain boundary. The highest Sb content inhibited the formation of IMCs resulting in the increased formation of small particle pinning of $\text{Ag}_3(\text{Sn,Sb})$ along the grain boundary. Moreover, the addition of Sb to SAC305 solder alloy could increase the activation energy and thus reduce the atomic diffusion rate, inhibiting the excessive growth of IMCs.^[12,13,25] Therefore, the optimal concentration of Sb in these alloys is found to be 3.0 wt pct because the microstructure and the ultimate tensile strength of SAC305 solder alloys were both improved. These results are consistent with those reported for the additions of 1.0 to 2.0 wt pct Sb into Sn-3.5Ag solder alloys^[17] and 0.5 to 1.5 wt pct Sb into Sn-9Zn-0.5Al solder alloys.^[24]

2. Fracture surface

The microstructures of tensile test specimens are shown in Figure 5. The fracture surface of SAC305 shows numerous spherical dimples separated by thin walls on a ductile fractured surface. This pattern usually indicates that ductile fracture under tension is preceded

by a localized reduction in the cross-sectional area, called necking, as shown in Figure 5(a) and (b). However, adding 3.0 wt pct Sb to SAC305 solder alloys produced the brittle, fractured surface shown in Figure 5(c) and (d). This alteration to the fracture surface was caused by hard, brittle phases of IMCs on the grain boundary of the β -Sn matrix, which sharply reduced the separated spherical dimples on the fracture surface as a result of the reduced elongation of the SAC305 solder alloy.

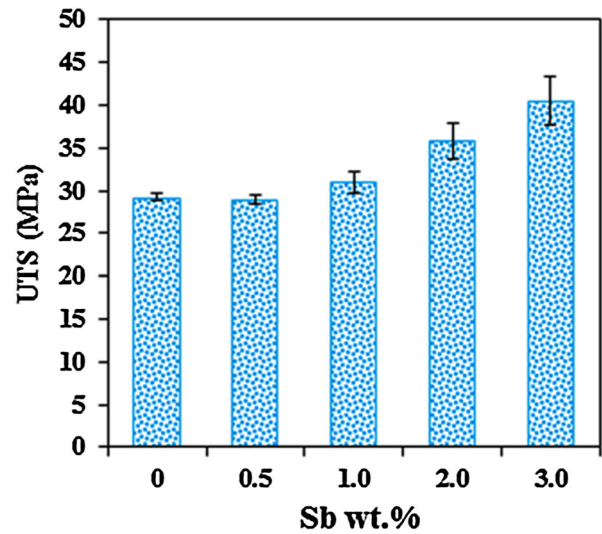


Fig. 3—Ultimate tensile strength of the solder alloys.

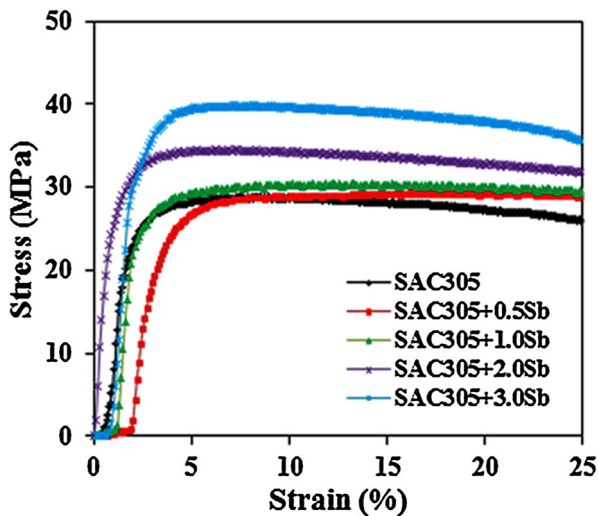


Fig. 2—Stress to strain curves of the solder alloys.

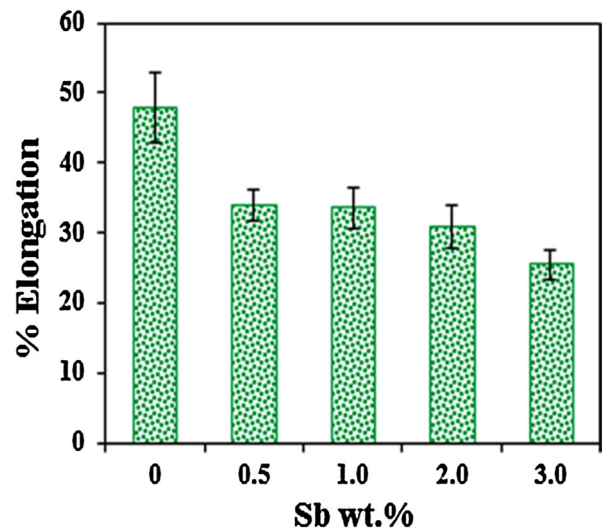


Fig. 4—Elongation (pct) of the solder alloys.

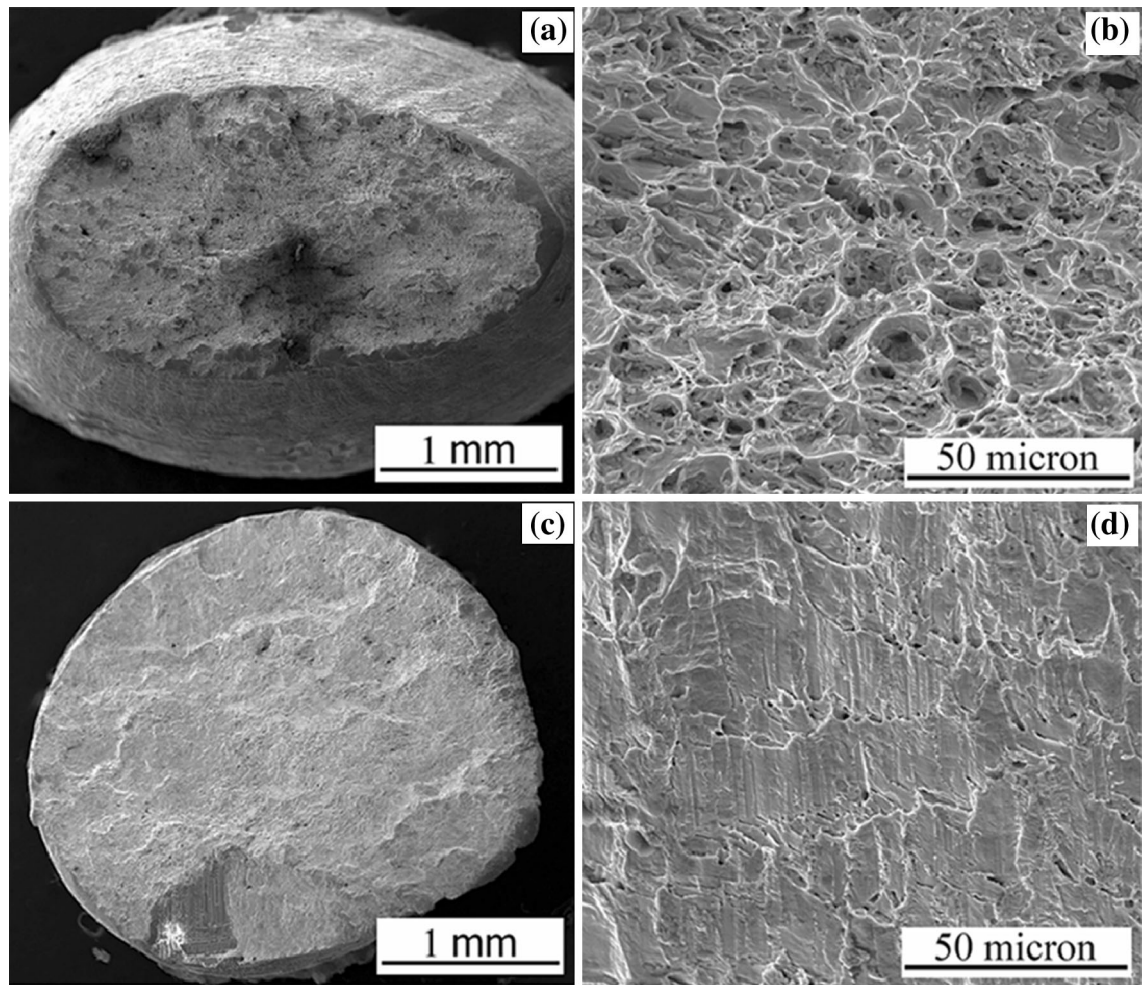


Fig. 5—Fracture surfaces of tensile specimens: (a) and (b) SAC305, and (c) and (d) SAC305 + 3.0Sb.

B. Microstructures of Solder Alloys

1. SEM analysis

Figure 6 shows the microstructures of the as-cast SAC305 solder alloys with different Sb contents. The microstructure of the initial SAC305 solder alloys is composed of intermetallic compounds (IMCs) such as Ag_3Sn and Cu_6Sn_5 ,^[26,27] and Figure 6(a) shows the microstructures of the β -Sn phase and IMCs phase (Ag_3Sn , Cu_6Sn_5) of these initial SAC305 solder alloys. The addition of Sb elements to the as-cast SAC305 solder alloys resulted in the formations of new $\text{Ag}_3(\text{Sn,Sb})$ and $\text{Cu}_6(\text{Sn,Sb})_5$ IMCs, as shown in Figure 6(b), (c), (d), and (e). The addition of greater amounts of Sb resulted in the formation of SnSb and increase in small particle pinning of $\text{Ag}_3(\text{Sn,Sb})$ along the grain boundary of the IMCs as a result of the inhibition of the growth of the IMCs, as shown in Figure 6(e).^[12,13,25] The original IMCs of SAC305 solder

alloy (Ag_3Sn and Cu_6Sn_5) are of brittle phase and of low ductility, properties that affect thermal fatigue lifetime and impair the mechanical properties of solder joints when soldering on a Cu substrate.^[12,14] The new solder alloy could inhibit the growth of IMCs and decrease the interdiffusion of elements due to the increased pinning on the grain boundary. Therefore, it could improve the mechanical properties of solder joints.^[12,14] EDX analysis confirmed that the β -Sn phase contained Ag_3Sn , Cu_6Sn_5 , SnSb, $\text{Cu}_6(\text{Sn,Sb})_5$, and small particle pinning of $\text{Ag}_3(\text{Sn,Sb})$.

2. EDX analysis

Figure 7 shows EDX mapping images of the elemental distribution in the SAC305 solder alloys. The green and pink areas are Ag and Cu phases uniformly interspersed along β -Sn phases (red areas). Figure 8 shows the distributions of Sn, Ag, Cu, and Sb elements

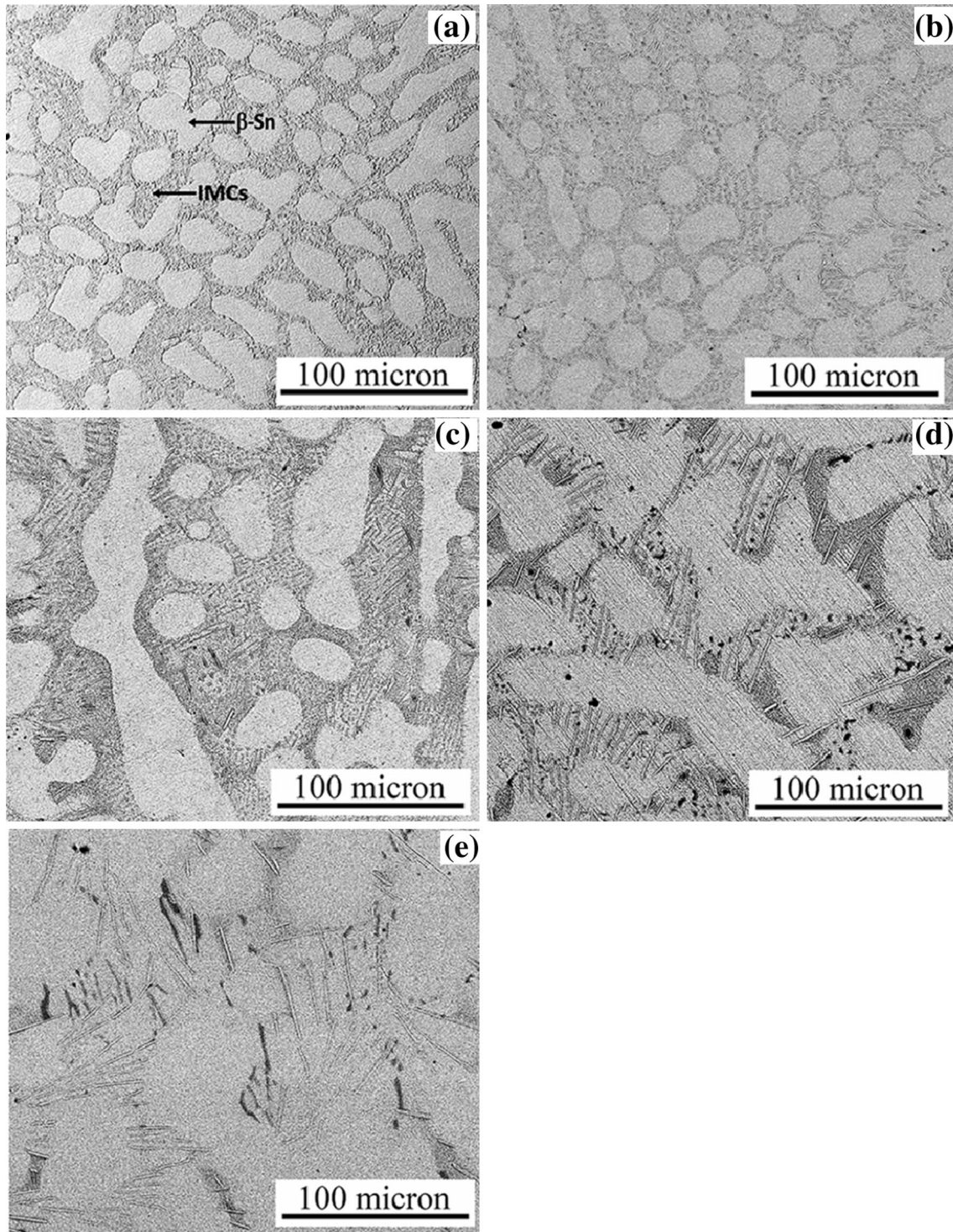


Fig. 6—SEM images at 500x of SAC305 solder alloys for different wt pct of Sb: (a) 0 pct, (b) 0.5 pct, (c) 1.0 pct, (d) 2.0 pct, and (e) 3.0 pct.

of SAC305 + 3.0Sb solder alloys. The red areas are Sn phases, the green areas are Ag phases, the pink areas are Cu phases, and the yellow areas are Sb phases distributed in the IMCs and Sn matrix phase. Figure 9

represents the phase compositions of SAC305 and SAC305 + 3.0Sb solder alloys. Only the IMCs of Ag_3Sn and Cu_6Sn_5 were observed in the SAC305 solder alloys, and the ratios of the composition of

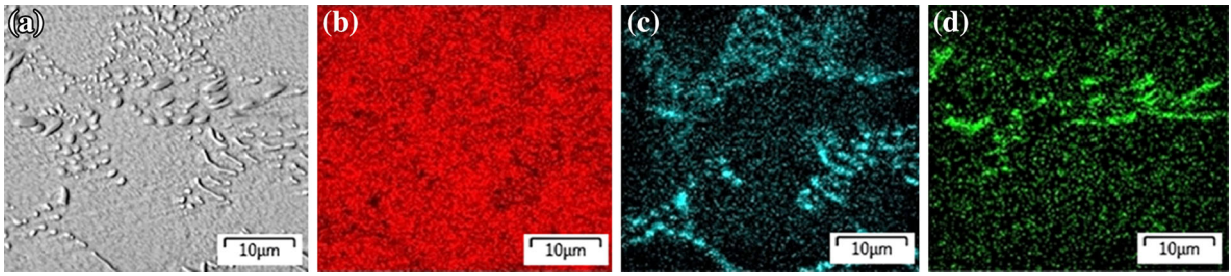


Fig. 7—EDX mapping images of elemental distribution: (a) SAC305, (b) Sn, (c) Ag, and (d) Cu.

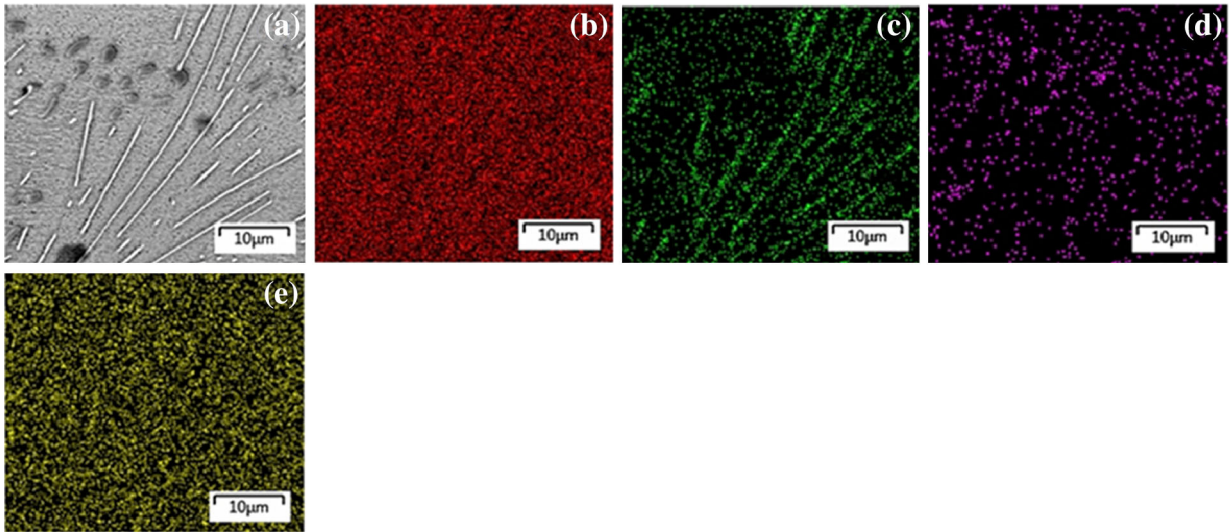


Fig. 8—EDX mapping images of elemental distribution: (a) SAC305 + 3.0Sb, (b) Sn, (c) Ag, (d) Cu, and (e) Sb.

these intermetallics, shown in Figure 9(a) and (b), were 71.1 wt pct Ag:28.9 wt pct Sn, and 35.8 wt pct Cu:64.2 wt pct Sn.^[25,26]

The compositions of the intermetallics from EDX analysis of the formations of SnSb, $\text{Cu}_6(\text{Sn,Sb})_5$ and $\text{Ag}_3(\text{Sn,Sb})$ in SAC305 + 3.0Sb solder alloys are shown in Figure 9(c) and (e). These compositions were 98.1 wt pct Sn:1.9 wt pct Sb; 25.2 wt pct Cu:73.1 wt pct Sn:1.7 wt pct Sb, and 40.2 wt pct Ag:58.1 wt pct Sn:1.7 wt pct Sb.^[12,13] These results are summarized in Table II. The higher Sb contents in SAC305 solder alloys resulted in the increased formation of small particle pinning of $\text{Ag}_3(\text{Sn,Sb})$ along the grain boundary as a result of inhibition of the formation of IMCs, and this can improve the mechanical properties of SAC305 solder alloys.^[13,14,28]

C. Thermal Behavior of Solder Alloys

The melting temperature of solder alloys is an important parameter in the soldering process. The melting temperatures of the experimental solder alloys were determined by DSC thermograms. Figure 10 shows the thermal properties of the five solder alloys during heating. The DSC results are summarized in Table III. The melting temperature of SAC305 solder alloys increased with the increasing Sb content. Figure 10 shows only one endothermic peak, at 495.7 K (222.7 °C), for the eutectic point of SAC305 solder alloy. This is consistent with previous data reported for the melting process of SAC305 solder alloys.^[29,30] For the Sb-containing solders, single endothermic peaks are present at 496.1 K, 498.0 K, 499.2 K, and 499.9 K (223.1 °C, 225.0 °C, 226.2 °C,

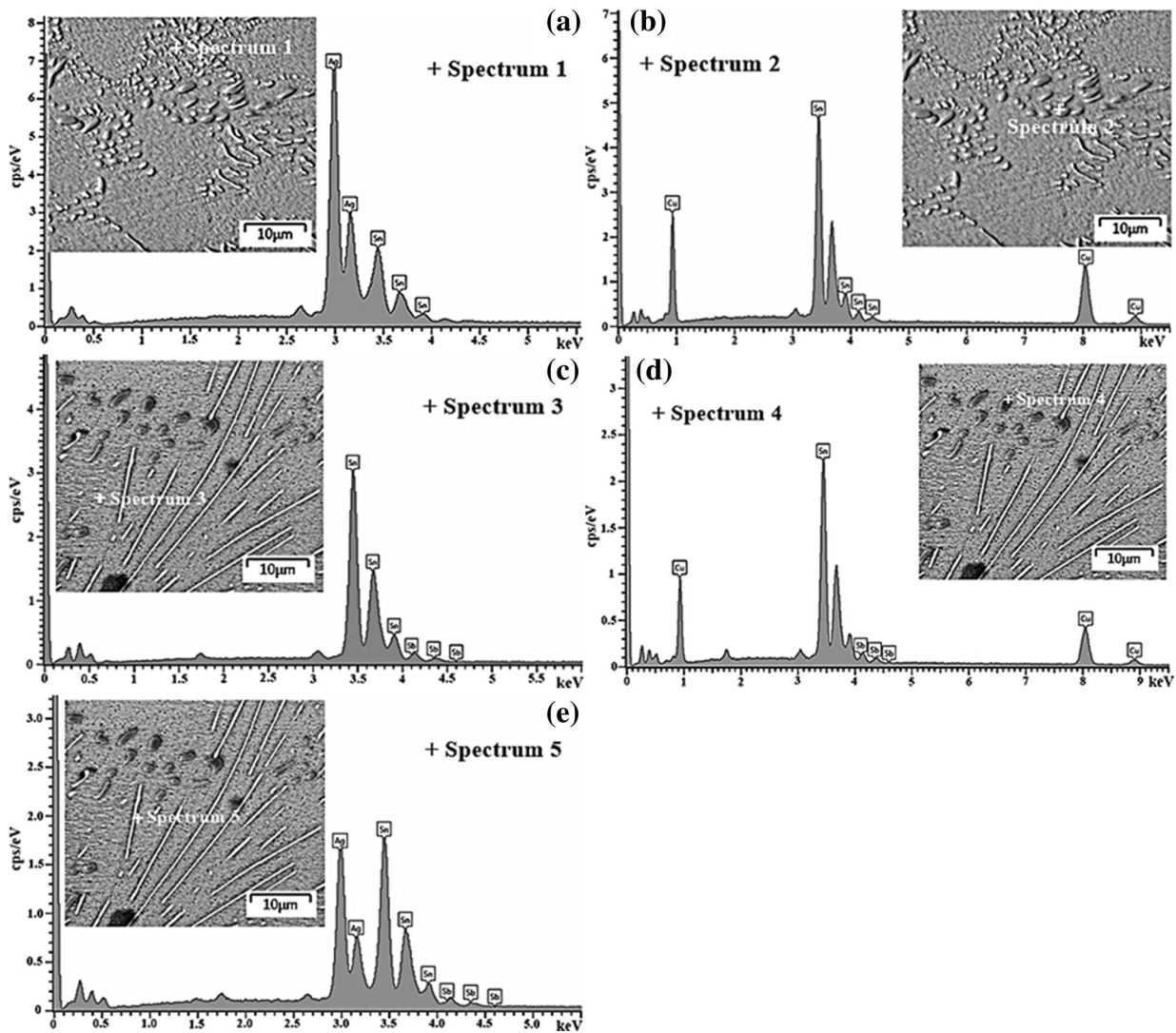


Fig. 9—SEM-EDX analysis of intermetallic compounds (IMCs) on grain boundaries of (a) and (b) SAC305 and (c) to (e) SAC305 + 3.0Sb.

Table II. The Chemical Compositions of SAC305 and SAC305 + 3.0Sb Alloys Measured by EDX (Weight Percent)

| Elements | Spectrum 1 Ag ₃ Sn | Spectrum 2 Cu ₆ Sn ₅ | Spectrum 3 SnSb | Spectrum 4 Cu ₆ (Sn,Sb) ₅ | Spectrum 5 Ag ₃ (Sn,Sb) |
|----------|----------------------------------|---|--------------------|--|---------------------------------------|
| Sn | 28.9 | 64.2 | 98.1 | 73.1 | 58.1 |
| Ag | 71.1 | — | — | — | 40.2 |
| Cu | — | 35.8 | — | 25.2 | — |
| Sb | — | — | 1.9 | 1.7 | 1.7 |

and 226.9 °C) for SAC305 + 0.5Sb, SAC305 + 1.0Sb, SAC305 + 2.0Sb, and SAC305 + 3.0Sb solder alloys, respectively. The melting point of Sb-containing solder alloys was higher [277.2 K (4.2 °C)] due to the formation of a new eutectic phase of (Ag₃(Sn,Sb), Cu₆(Sn,Sb)₅). However, Table III shows that the addition ranging from

0.5 to 3.0 wt pct Sb elements to the SAC305 solder alloy slightly increased both the solidus [T_{onset} , 496.4 K (223.4 °C)] and liquidus temperatures [T_{end} , 502.9 K (229.9 °C)]. These results are consistent with previous reports of Sn-3.5Ag and SAC105 solder alloys.^[17,20] Moreover, the pasty range values of the SAC305,

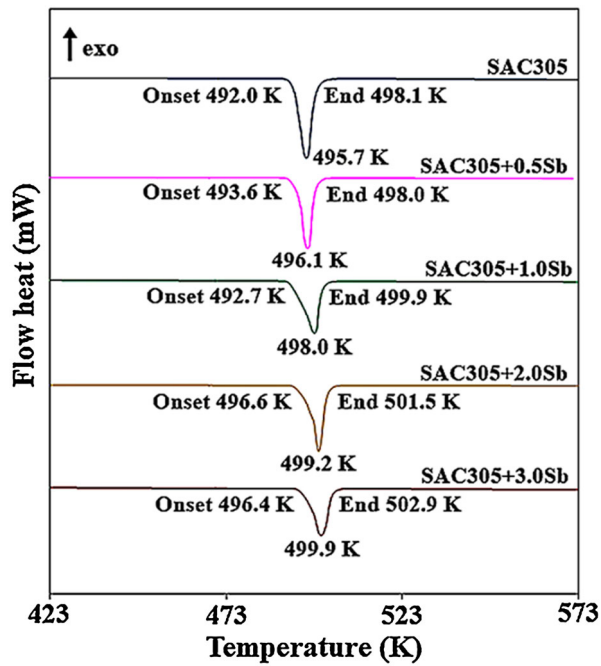


Fig. 10—DSC results of the solder alloys during heating.

SAC305 + 0.5Sb, SAC305 + 1.0Sb, SAC305 + 2.0Sb, and SAC305 + 3.0Sb solder alloys are 279.1 K, 277.4 K, 280.2 K, 277.2 K, and 279.0 K (6.1 °C, 4.4 °C, 7.2 °C, 4.9 °C, and 6.5 °C) which are all lower than the value of 284.5 K (11.5 °C) for the Sn-37Pb eutectic.^[31,32] It was observed that the addition of Sb elements did not significantly affect the pasty range of SAC305 solder alloys.

IV. CONCLUSIONS

Antimony has been added to SAC solder alloys in efforts to overcome a few of their shortcomings. This study of the effects of this addition on the microstructural, mechanical, and thermal properties of SAC305 alloys showed that its addition led to microstructural improvements, a more uniform distribution of the IMCs, and the formations of new $Ag_3(Sn,Sb)$ and $Cu_6(Sn,Sb)_5$ IMCs on the grain boundary of the β -Sn phase. The highest Sb content resulted in the formation of SnSb and small particle pinning of $Ag_3(Sn,Sb)$ along the grain boundary of the IMCs. The alloys' ultimate tensile strength increased, and their ductility decreased as a function of their Sb content. Analysis of the alloys' thermal properties showed that the alloys containing Sb had slightly higher melting points than SAC305 and that the pasty range of the SAC305 solder alloy was not significantly changed by additions of Sb from 0.5 to 3.0 wt pct. Adding Sb improved both the ultimate tensile strength and the microstructure of the SAC305 solder alloys and, in these respects, 3.0 wt pct Sb had the best outcome of all the antimony additions studied in this research.

Table III. Comparison of Solidus Temperature (T_{onset}) and Liquidus Temperature (T_{end}) of Solder Alloys from DSC Heating Curves

| Solder Alloys | T_{onset} [K(°C)] | T_{end} [K(°C)] | Pasty Range ($T_{end}-T_{onset}$) [K (°C)] | Melting Temperature [K (°C)] |
|----------------|---------------------|-------------------|--|---------------------------------|
| Sn-37Pb | 452.5 (179.5) | 464.0 (191.0) | 284.5 (11.5) | 456.0 (183.0)[51] |
| SAC305 | 492.0 (219.0) | 498.1 (225.1) | 279.1 (6.1) | 495.7 (222.7) |
| SAC305 + 0.5Sb | 493.6 (220.6) | 498.0 (225.0) | 277.4 (4.4) | 496.1 (223.1) |
| SAC305 + 1.0Sb | 492.7 (219.7) | 499.9 (226.9) | 280.2 (7.2) | 498.0 (225.0) |
| SAC305 + 2.0Sb | 496.6 (223.6) | 501.5 (228.5) | 277.2 (4.9) | 499.2 (226.2) |
| SAC305 + 3.0Sb | 496.4 (223.4) | 502.9 (229.9) | 279.0 (6.5) | 499.9 (226.9) |

ACKNOWLEDGMENTS

This work has been supported by the Prince of Songkla University Research Fund (Fiscal Year 2016) under the Contract Number SCI590647. In addition, we would like to thank academician Thomas Duncan Coyne for his useful comments and effective language editing of the text in the manuscript.

REFERENCES

1. A.A. El-Daly and A.E. Hamdmad: *J. Alloys Compd.*, 2011, vol. 509, pp. 8854–60.
2. S.Y. Chang, C.C. Jain, T.H. Chuang, L.P. Feng, and L.C. Tsao: *Mater. Des.*, 2011, vol. 32, pp. 4720–27.
3. H.R. Kotadia, O. Mokhtari, M.P. Clode, M.A. Green, and S.H. Mannan: *J. Alloys Compd.*, 2012, vol. 511, pp. 176–88.
4. A.A. El-Daly, A. Fawzy, A.Z. Mohamad, and A.M. EL-Taher: *J. Alloys Compd.*, 2011, vol. 509, pp. 4574–82.
5. L. Zhang, S.B. Xue, G. Zeng, L.L. Gao, and H. Ye: *J. Alloys Compd.*, 2012, vol. 510, pp. 38–45.
6. F. Lin, W. Bi, G. Ju, W. Wang, and X. Wei: *J. Alloys Compd.*, 2011, vol. 509, pp. 6666–72.
7. F. Zhu, H. Zhang, R. Guan, and S. Liu: *J. Alloys Compd.*, 2007, vol. 438, pp. 100–05.
8. L. Gao, S. Xue, L. Zhang, Z. Sheng, F. Ji, and W. Dai: *Microelectron. Eng.*, 2010, vol. 87, pp. 2025–34.
9. A.K. Gain, Y.C. Chan, and W.K.C. Yung: *Microelectron. Reliab.*, 2011, vol. 51, pp. 975–84.
10. T. Ventura, S. Terzi, M. Rappaz, and A.K. Dahle: *Acta Mater.*, 2011, vol. 59 (4), pp. 1651–58.
11. R. Mahmudi and S. Mahin-Shirazi: *Mater. Des.*, 2011, vol. 32, pp. 5027–32.
12. B.L. Chen and G.Y. Li: *Thin Solid Films*, 2004, vols. 462–463, pp. 395–401.
13. BL Chen and GY Li: *IEEE Trans. Compon. Packag. Technol.*, 2005, vol. 28 (3), pp. 534–41.
14. G.Y. Li, B.L. Chen, and J.N. Tey: *IEEE Trans. Compon. Packag. Technol.*, 2004, vol. 27, pp. 77–85.
15. H.T. Lee, S.Y. Hu, T.F. Hong, and Y.F. Chen: *J. Electron. Mater.*, 2008, vol. 37 (6), pp. 867–73.
16. C.A. Handwerker, U. Kattner, and K.W. Moon: *Lead-Free Soldering*, 1st ed., Springer, US, 2007, p. 33.
17. H.T. Lee, M.H. Chen, H.M. Jao, and C.J. Hsu: *J. Electron. Mater.*, 2004, vol. 33 (9), pp. 1048–54.
18. I.E. Anderson, J.C. Foley, B.A. Cook, J.L. Haringa, R.L. Terpstra, and O. Unal: *J. Electron. Mater.*, 2001, vol. 30, pp. 1050–59.
19. K.W. Moon, W.J. Boettinger, U.R. Kattner, F.S. Biancaniello, and C.A. Handwerker: *J. Electron. Mater.*, 2000, vol. 29 (10), pp. 1122–36.
20. A.A. El-Daly, A.E. Hammad, A. Fawzy, and D.A. Nasrallah: *Mater. Des.*, 2013, vol. 43, pp. 40–49.
21. G.Y. Li, B.L. Chen, Z.Q. Shi, C.K. Stephen, and Z.F. Wang: *Thin Solid Films*, 2006, vol. 504, pp. 421–25.
22. K.S. Kim, S.H. Huh, and K. Sukanuma: *Microelectron. Reliab.*, 2003, vol. 43 (2), pp. 259–67.
23. V.L. Nguyen, C.S. Chung, and H.K. Kim: *Microelectron. Reliab.*, 2015, vol. 55, pp. 2808–16.
24. A.B. El Basaty, A.M. Deghady, and E.A. Eid: *Mater. Sci. Eng. A*, 2017, vol. 701, pp. 245–53.
25. B.L. Chen and G.Y. Li: *Proc. Electron. Compon. Technol., Louisiana*, 2003, pp. 1235–42.
26. K. Kanlayasiri, M. Mongkolwongrojn, and T. Ariga: *J. Alloys Compd.*, 2009, vol. 485, pp. 225–30.
27. A.A. El-Daly, F. El-Tantawy, A.E. Hammad, M.S. Gaafar, E.H. El-Mossalamy, and A.A. Al-Ghamdi: *J. Alloys Compd.*, 2011, vol. 509, pp. 7238–46.
28. A. Fawzy, S.A. Fayek, M. Sobhy, E. Nassr, M.M. Mousa, and G. Saad: *Mater. Sci. Eng. A*, 2014, vol. 603, pp. 1–10.
29. Z.B. Luo, J. Zhao, Y.J. Gao, and L. Wang: *J. Alloys Compd.*, 2010, vol. 500, pp. 39–45.
30. L.W. Lin, J.M. Song, Y.S. Lai, Y.T. Chiu, N.C. Lee, and J.Y. Uan: *Microelectron. Reliab.*, 2009, vol. 49, pp. 235–41.
31. A.A. El-Daly, Y. Swilem, and A.E. Hammad: *J. Alloys Compd.*, 2009, vol. 471, pp. 98–104.
32. A.A. El-Daly and A.E. Hammad: *J. Alloys Compd.*, 2010, vol. 505, pp. 793–800.